Mutagenesis of Some Positive and Negative Residues Occurring in Repeat Triad Residues in the ADP/ATP Carrier from Yeast†

Veronika Müller,‡ Dörthe Heidkämper,‡ David R. Nelson,§ and Martin Klingenberg*,‡

Institute of Physical Biochemistry, University of Munich, Schillerstrasse 44, 80336 Munich, Germany, and Department of Biochemistry, The University of Tennessee, Memphis, Tennessee 38163

Received July 30, 1997; Revised Manuscript Received October 17, 1997⊗

ABSTRACT: In AAC2 from *Saccharomyces cerevisiae*, nine additional charged residues (six positive, three negative) were neutralized by mutagenesis following the previous mutation of six arginines. Oxidative phosphorylation (OxPhos) in cells and mitochondria, the expression level of AAC protein, and the various transport modes of AAC in the reconstituted system were measured. Mutations are: within the first helix at K38A which is exclusive for AAC; K48A, and R152A, part of a positive triad occurring in the matrix portion of each repeat; two matrix lysines, K179M and K182I, and the negative triad helix-terminating residues, E45G, D149S, D249S. Cellular ATP synthesis (OxPhos) is nearly completely inhibited in K48A, R152A, D149S, and D249S, but still amounts to 10% in K38A and between 30% and 90% in the gly$^+$ mutants K179M, K179I + K182I, and E45G. Comparison of the AAC content measured by ELISA and the binding of [^{3}H]CAT and [^{3}H]BKA reveals discrepancies in K48A, D149S, and D249S mitochondria, which provide evidence that these mutations largely abolish inhibitor binding. Also these mitochondria have undetectable OxPhos. Differently in K38A, CAT and BKA binding are retained at high AAC levels but OxPhos is very low. This reveals a special functional role of K38, different from the more structural role of R152, K48, D149, and D249. Transport activity was measured with reconstituted AAC. The electroneutral ADP/ADP exchange of gly$^-$ mutants is largely or fully suppressed in K48A, D149S, and D249S. K38A and R152A are still active at 18% and 30% of wt. The other three exchange modes, ATP/ADP, ADP/ATP, and ATP/ATP, are nearly suppressed in all gly$^-$ mutants but remain high in gly$^+$ mutants. ATP-linked modes are higher than the ADP/ADP mode in gly$^+$ but lower in gly$^-$ mutants, resulting in an exchange mode inversion (EMI). In the competition for AAC2 transport capacity, the weak ATP exporting modes are suppressed by the much stronger unproductive ADP/ADP mode causing inhibition of OxPhos. Together with previous results all members of three charge triads are now mutagenized, revealing drastic functional rotatory asymmetries within the three repeat domains. In the intrahelical arginine triad the third (R294A), in the positive matrix triad the second (R152A), and in the helix-terminating negative triad the first (E45G) still show high activity.

ADP/ATP carrier (AAC)[1] provides the terminal step of mitochondrial oxidative phosphorylation (OxPhos) by actively exporting ATP into the cytosol coupled with the import of ADP into the mitochondrial matrix. For this function mitochondria contain high amounts of this membrane protein (*1*) which facilitated the first isolation of an intact biomembrane transporter (*2*). The AAC is a member of the mitochondrial carrier family and it was the first protein of this family where common structural characteristics were identified (*3*). The proteins comprise about 300−320 residues which are assumed to be folded through the membrane with six helices. A striking feature is the partition of the total sequence into three similar repeat domains of about 100 residues, each of which contain two transmembrane helices (*4*, *5*). In each domain on the matrix side, a hydrophilic stretch about 40−45 residues long connects the two transmembrane helices. Several clusters of charged residues are well conserved between these three domains. The isolated intact AAC exists as a homodimer with binding only one molecule of the inhibitor ligands or substrates ADP and ATP (*6*).

A systematic analysis of the structure/function relationships within the AAC was initiated on the AAC2 of *Saccharomyces cerevisiae*. For this purpose *S. cerevisiae* strains were prepared lacking the isoforms AAC1 and AAC2 and used as host for plasmids carrying AAC2 mutations (*7*). Most mutations were selected in conserved polar residues at conspicuous locations. They have been screened for a defect in AAC by growth on the nonfermentable carbon source glycerol. In further work, the defects were quantitatively assayed by biochemical determinations at the level of cells, mitochondria, and the isolated and reconstituted AAC. First, mutants in which six conspicuously located arginines were converted into neutral residues were functionally scrutinized (*8*, *9*). These mutations caused defects by suppressing protein expression and by altering ATP and ADP transport preferences. As a rule, a neutralization of these arginines had a significant impact on the translocation of the more highly charged ATP^{4-} than of ADP^{3-}, indicating electrostatic

† This work was supported by grants from Deutsche Forschungsgemeinschaft (Kl 134/32-1) and from NATO and National Institutes of Health Grant HL54248 (to D.R.N.).

* Address correspondence to this author. Tel: +49-89-5996473. FX: +49-89-5996415.

‡ University of Munich.

§ The University of Tennessee.

⊗ Abstract published in *Advance ACS Abstracts,* December 1, 1997.

[1] Abbreviations: AAC, ADP/ATP carrier; BKA, bongkrekate; CAT, carboxyatractylate; EMI, exchange mode inversion; OxPhos, oxidative phosphorylation; wt, wild type; p-wt, plasmid carrying wt AAC.

S0006-2960(97)01867-9 CCC: $14.00

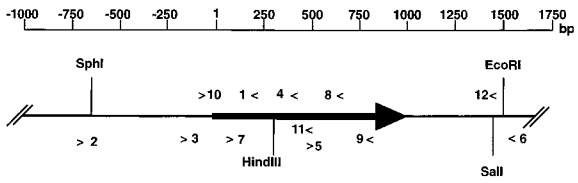

FIGURE 1: Primers used in mutgenesis of AAC2. The gene resides on plasmid pSEYc58. *Sph*I and *Eco*RI are part of the polylinker region. Forward primers are indicated by >, reverse primers by <. Bases are numbered from the ATG start site of AAC2.

interactions of these arginines in the translocation path. The comparison of OxPhos rates in isolated wt and mutant mitochondria and cells revealed how the intracellular competition by ATP and ADP for the AAC regulates OxPhos in mutants, due to the decrease of ATP versus ADP transport capability.

In the present work the mutations of some further charged residues into neutral ones are studied on three levels, cells, mitochondria, and reconstituted AAC. They are, with one exception, part of residue triads located at homologous position in the three repeat domains. They thus complement and extend the previously described crop of six arginine mutants. The quantitative biochemical analysis of the mutational effects reveals striking effects, such as exchange mode inversion (EMI) and triad asymmetry with important structure/function and regulatory implications.

MATERIALS AND METHODS

Yeast Strains and AAC2 Mutants. The K179M mutant and the K179I + K182I double mutant were made by the method of Zoller and Smith (*11*) as reported in ref *7*. The mutagenic primer 5′GATGTCTACAAGAt(g/t)ACCTTAAt-(g/t)TCTGATGGTGTTGC3′ was degenerate so either Met or Ile codons would replace the Lys codons. Lower case letters indicate mutated bases. The intent was to replace the positive Lys side chains with hydrophobic alternatives. Only two of the eight possible combinations of mutants were isolated.

E45G (GAA to GGA) was a revertant mutation from the parent R294A. This mutation was isolated from the R294A mutation on an *Sph*I *Hin*dIII fragment that was spliced into a wild type AAC2 background to give the separate E45G mutation.

The five mutants K38A, K48A, R152A, D149S, and D249S were all made using PCR. K38A was described previously (*10*). The location of primers used in the mutagenesis is shown in Figure 1. K48A was made using primer 1 (154 5′GGATCAAAAGTgcAACTCTTTCG3′ 132) with primer 2 (the M13-40 primer) to produce an 829 bp fragment. Primer 3 (−173 5′TTTTCACGACAACCCACTC3′ −155) and primer 4 (372 5′GGCCTAACCTTCTTCCT-TCT3′ 353) amplified an overlapping 545 bp fragment, including the *Hin*dIII site. These two PCR products were combined in a third PCR reaction with primers 2 and 4. The overlapping fragments annealed and were extended and amplified to form a 1047 bp fragment. This fragment was cut with *Sph*I and *Hin*dIII and ligated into a wild type AAC2 background to make the K48A mutant.

The three mutants D149S, R152A, and D249S were made with a similar strategy. The R152A mutagenic primer 5 (444 5′GGATTATGCAgcAACTAGATTGGC3′ 467) was used with primer 6 (M13-24 reverse primer) to make a 1075 bp fragment with an *Eco*RI site near the 3′ end. Primer 7 (100 5′GCCGCTGTCGCCgctACTGCTGCATCTCC3′ 128, the K38A mutagenic primer) and primer 8 (568 5′AAAAGAC-CAGCAACACCATCA3′ 549) amplified an overlapping 469 bp fragment that included the *Hin*dIII site. The two fragments were combined as above with the outside primers 6 and 7 to make a 1419 bp fragment that was cut with *Hin*dIII and *Eco*RI and ligated into a wild type background to make the R152A mutant. In the process, the K38A mutation was cut off. D249S was made in essentially the same way with mutagenic primer 9 (755 5′CTAACGGTAc(c/t)CAATGGG-TAAGAAC3′ 731). This primer was degenerate in codon 249 so both glycine (GGT) and serine (AGT) codons could be made at this site. The forward primer for this PCR reaction was primer 10 (−12 5′AAGagAtctGCCATGTCT-TCTAACGCCC3′ 16, originally used to introduce a *Bgl*II site upstream of AAC2). The product of this reaction was 767 bp. An overlapping fragment (1419 bp) was made with primers 6 and 7. The product of the third PCR reaction (1530 bp) that joined the two overlapping fragments was made using the outside primers 6 and 10. It was cut with *Hin*dIII and *Eco*RI and ligated into a wild type AAC2 background. The D149S mutant was made using primer 11 (455 5′CTTGCATAAc(c/t)CAAAGAGTAAAC3′ 433) with primer 7 to make a 356 bp product, including the *Hin*dIII site. The fragment was designed to contain D149S or D149G mutations. A *Hin*dIII *Eco*RI fragment from AAC2 was used as the second overlapping fragment. This contained the 3′ end of AAC2 and a *Sal*I site near the 3′ end. A second PCR reaction combined these two fragments with primer 7 and primer 12 (1456 5′CGTTCTCTAGGTCGACGTC3′ 1438) that contains the naturally occurring *Sal*I site (underlined). The PCR product of this reaction was cut with *Hin*dIII and *Sal*I and ligated into a wild type AAC2 background. All mutants were sequenced to confirm the mutations and check for PCR errors.

Isolation of Cells and Mitochondria. The maintenance and control of the yeast strains were performed as described previously (*8*). **Cells** were grown on large-scale culture of 24 L in a complete medium containing for the gly^+ strain 2% lactate and for the gly^- strains 1% galactose. Details were described previously (*8*). **Mitochondria** were isolated as described (*8*).

Oxidative phosphorylation in cells in isolated mitochondria was measured by following the kinetics of ATP function. These measurements followed the procedure previously introduced (*8*). For determining the portion of OxPhos which passed through the AAC, in a parallel experiment BKA was added to the yeast cells, the combined BKA and CAT were added to mitochondria, and the ATP was measured after 150 s. The inhibitor sensitive (corrected) OxPhos rate was calculated according to the formula

$$V_{ATP}^{corrected} = V_{ATP}(1 - [ATP(+BKA)]/[ATP])$$

where V_{ATP} is the total rate without inhibitor and [ATP] and [ATP (+BKA)] are the amounts of ATP found without and with BKA 150 s after the start of OxPhos. See also the method section in ref *8*.

The **AAC content** in mitochondria was determined by ELISA assay as previously described (*8*). Measurements of [^{3}H]CAT and [^{3}H]BKA binding to mitochondria were performed as desribed (*8*).

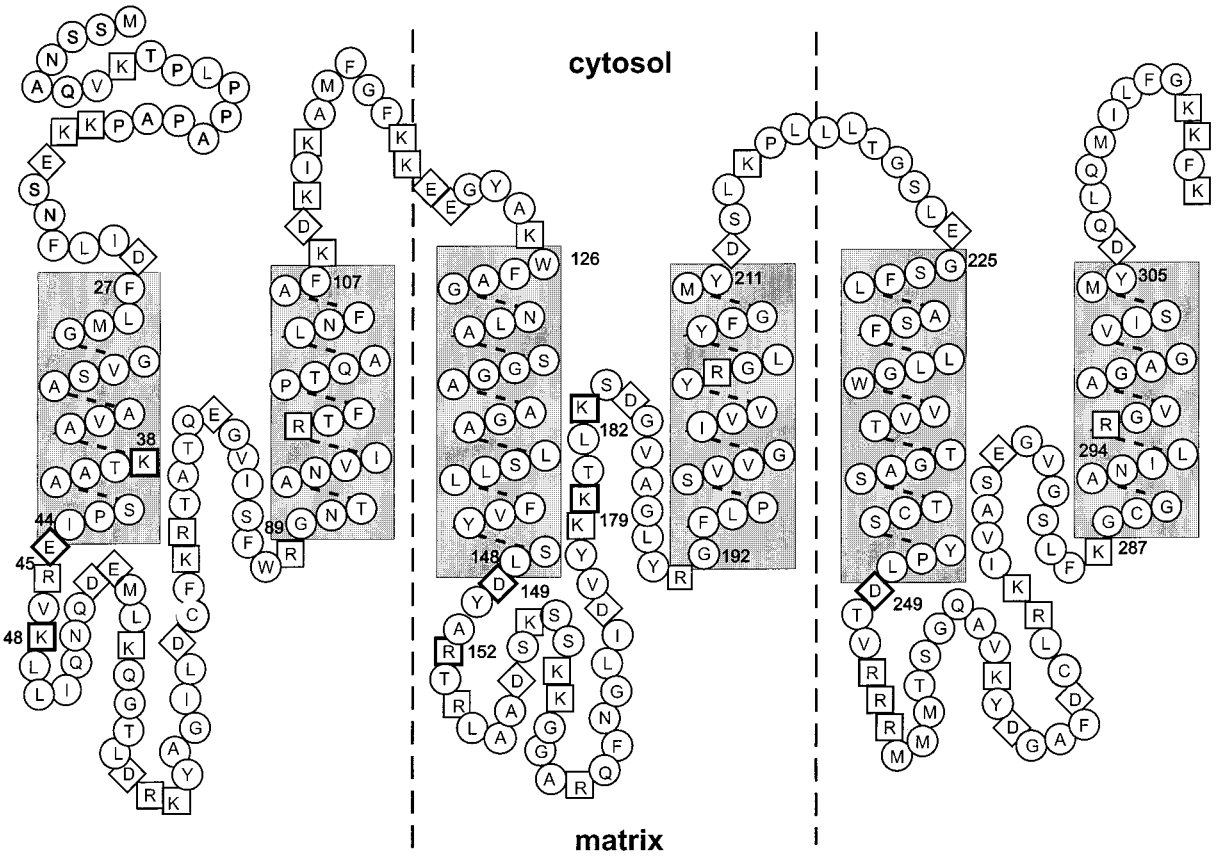

FIGURE 2: Localization of mutations in the AAC2 from *S. cerevisiae*. The AAC is folded according to the three repeat structure with six transmembrane helices shown in shaded blocks. The frames around the residues signify (◇) negative, (□) positive, (○) neutral residues.

The **isolation of AAC** from mitochondria and the **reconstitution** into phospholipid vesicles of AAC were performed as described (*9*). **The exchange rates** were measured according to the rapid mixing and removal procedure as described (*9*). The exchange rates were evaluated to a first-order rate law using a computerized program (*9*).

RESULTS

Selection of Mutants. The selection of residues for mutagenesis is based on a folding model of the AAC2, in which six transmembrane helices traverse the membrane. They are connected on the matrix side by three hydrophilic stretches of about 40 residues (Figure 2). Only polar residues were selected for mutation with the following guidelines.

(a) Basic Residues. The unusual K38 in the first helix occurs at similar positions in all AAC structures (*12*). It is not found at homologous positions in any other member of the mitochondrial carrier family. Formerly, in bovine heart mitochondria the accessibility of lysines were probed using the membrane impermeant lysine reagent pyridoxal phosphate. The homologous K24 was accessible from the cytosolic site and the only lysine in the AAC which was completely protected by carboxyatractylate (CAT) against Schiff-base formation with pyridoxal phosphate (*13*). Therefore it was suggested that K38 plays a specific role in the binding center and is also involved in translocation. In the hydrophilic matrix regions two positive residues K48 and R152 were targeted which are part of the motif (+x+) occurring in each of the three repeat domains on the matrix side, near the first helix. In the third domain this motif is expressed as RRR and its mutants have been characterized in a previous publication (*8*). Further, neutralizing mutations were targeted at K179 and K182. The mutation of K179 was motivated by the finding that the homologous K162 in bovine heart mitochondria reacted with pyridoxal phosphate from the cytosolic side, although according to the single folding model it is located at the matrix side (*13*). K162 reacted only when the carrier was brought into the m-state with BKA. This finding prompted us to propose that K162 is part of the translocation channel through which the pyridoxal phosphate can gain access to this residue. The possibility was discussed that K162 is located in a small loop protruding into the membrane together with similar loops in the two other domains.

(b) Acidic Residues. The last group encompasses three acidic residues, E45, D149, and D249, which are assumed to terminate the first helix in each domain on the matrix side. Elimination of the negative charge might destabilize the helix insertion into the phospholipid bilayer. Moreover, E45 was found in revertant selections (*14, 15*) to be a second-site revertant mutation of primarily 294A and K38A. Therefore, E45 and the homologous D149 and D249 were targeted also in view of their possible role in second-site revertants.

Oxidative Phosphorylation in Cells. For comparison, in all experiments the strain carrying the wild type AAC plasmid (p-wt) is included. In the screening for growth on nonfermentable glycerol, out of the eight mutants only three, E45G, K179M, and K179I + K182I, turned out to remain glycerol positive. In other words, we can expect a large mutational decrease of function in the AAC mutants K38A, K48A, R152A, D149S, and D249S so that the AAC does not sustain enough oxidative phosphorylation for growth on a nonfermentable source.

To make a quantitative assessment of the mutational effects on OxPhos, we determined the rate of ATP synthesis in these cells. First, the intracellular ATP was depleted by a 1 h

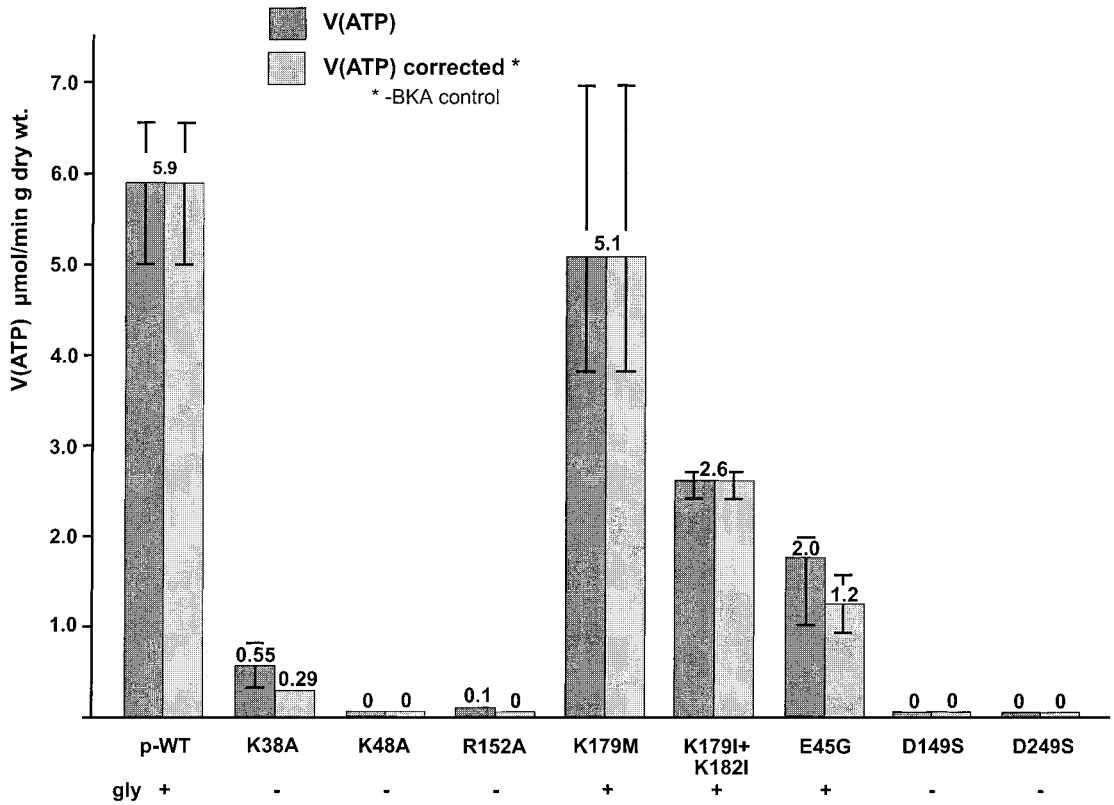

FIGURE 3: Oxidative phosphorylation in cells. The rates of ATP formation are given without and with correction for the BKA resistant rates. The ATP synthesis rate *V*(ATP) is evaluated from the time dependence of ATP formation (see Materials and Methods).

incubation under anaerobic conditions, and then ATP synthesis was started by oxygen addition in the presence of ethanol as a substrate. To control to which extent the ATP synthesis is mediated by the AAC, the AAC inhibitor BKA was used which can penetrate into the yeast cells. To facilitate the uptake of BKA, the cells had to be incubated at low pH (pH 5). The results are given in Figure 3 and include for comparison the phosphorylation rate of the plasmid wild type AAC-containing cells. In the K38 mutant cells the OxPhos rate was reduced to a level of only 10% of the wild type activity. But only half of this activity was inhibited by BKA and thus can be attributed clearly to AAC-linked activity. In K48A and in R152A only traces of phosphorylation activity can be detected. In the K179M mutant the phosphorylation rate is nearly the same as the wild type activity, and in the double mutant K179I + K182 it is reduced to slightly less than half.

The mutations of the three negative helix-terminating residues have quite divergent effects. Among the three mutants of the helix-terminating negatively charged residues E45G stands out for being gly^+, whereas D149S and D249S are gly^-. Accordingly, in the quantitative assessment of cellular phosphorylation capacity E45G retains 30% of wt activity, whereas D149S and D249S are virtually devoid of OxPhos activity.

Expression Level of AAC and Binding of AAC Inhibitors. The qualitative test by immuno blotting for the occurrence of AAC in mitochondria shows clear signals for AAC expression with all mutants, the poorest level being in D249S (Figure 4 inset). Variations in the stain, however, do not fully reflect the large differences of AAC content, as measured by the quantitative ELISA (Figure 4). According to ELISA, in most mutant mitochondria the AAC content still contains about half of wild type levels. The lowest contents of AAC are seen in R152A and D249S mutant mitochondria.

The binding of the specific inhibitors for AAC, carboxyatractylate (CAT), and bongkrekate (BKA) produces several pieces of information. A discrepancy between CAT and BKA binding and the quantitative ELISA would indicate that the mutation is important for the inhibitor binding site. Further, since CAT and BKA bind from opposite sides to the AAC (*16*), the binding of both inhibitors can be differently affected. The binding assays also can provide determinations of the AAC content that are more precise than the ELISA. In case the mutation causes a moderate decrease of the affinity, the binding capacity can still be measured by the excess concentration of CAT and BKA used.

In the majority of the mutants the binding values for CAT and BKA parallel the AAC content determination by ELISA (Figure 5) in K38A, K179I, K179I + K182I, E45G, and R152A. In the K38A mitochondria CAT binding reaches about 60% of the wild type and in the K179M and K179I + K182 mutants the CAT binding is reduced by only 30% and 50%. In R152A the low CAT binding of only 20% of wt corresponds to the low ELISA determined content. The BKA binding is mostly higher in these mitochondria than the CAT binding by a factor of about 1.25 which has also been noted in other mitochondria (*15*).

Very strong suppression of inhibitor binding is seen in the K48A and D149S and a virtual complete abolition in the D249S mutant. This contrasts to the ELISA determinations of the AAC protein, which measure still significant amounts of AAC protein in these mutant mitochondria. This discrepany indicates that each of these three mutations largely abolishes the binding of CAT and BKA. Concentration dependence of CAT binding (not shown) indicates that impairment is not due to a lowering of the binding affinity.

Oxidative Phosphorylation in Mitochondria. The respiratory capacity of mitochondria can be expected to be linked

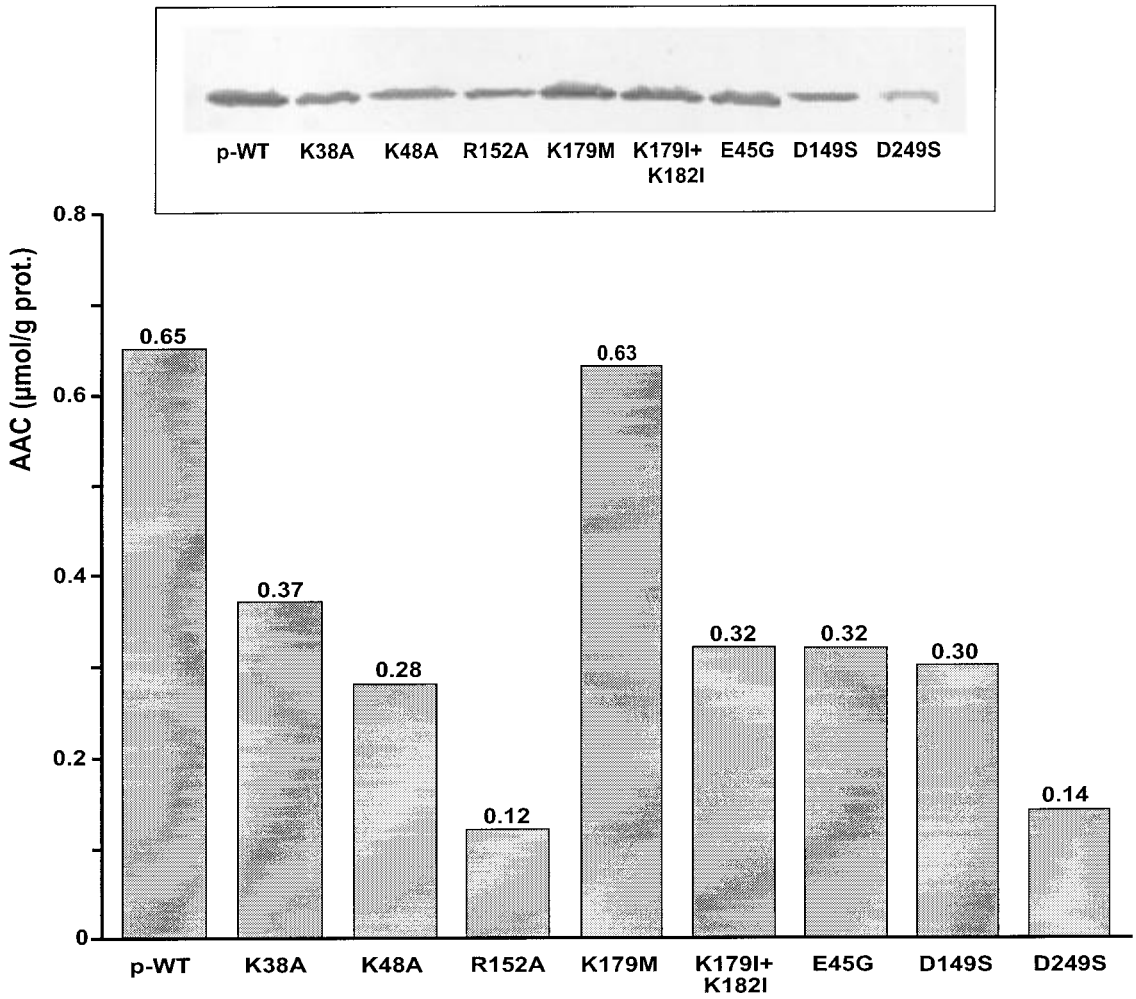

FIGURE 4: Content of AAC in the mitochondria from various AAC mutants as determined by competitive ELISA and immunoblots (inset). The range encompasses two−four values from different mitochondrial preparations. The content refers to the AAC dimer. For details see Materials and Methods.

to OxPhos capacity and thus also to the AAC activity and was determined by measuring the oxygen uptake rate with the substrate glycerol 1-phosphate. Further, the content of cytochrome *c* was measured. Cytochrome *c* was chosen since it can be accurately measured in mitochondria from mutants even with low expression levels of respiratory components. The results listed in Table 1 show that, where measured, all mutant mitochondria except D249S still exhibit a measurable respiration, although much lower in K48A and D149S. The cytochrome *c* content is quite resistant to mutations varying only from 0.3 to 0.5 μmol/g of protein. This is remarkable in view of the virtual absence of OxPhos in several mutants (K48, D149S, D249S) as shown below.

In mitochondria isolated from these cells the oxidative phosphorylation rate was measured with the hexokinase glucose trap system (Figure 6A). Also here the AAC-dependent portion of OxPhos was differentiated by the addition of BKA. In the K38A mutant mitochondria the OxPhos rate is reduced to about 4% of the wt rate, out of which only one-third is sensitive to BKA. As a result, this mutant has only 1% of wt AAC dependent OxPhos activity. In the K48A the activity is about 1% and cannot be inhibited by BKA. R152A has 8% of wt activity, half of which is inhibitable by BKA. Both the K179M mutant and the K179I + K182I double mutant exhibit activities equal to 120 or 50% of wt respectively. When OxPhos activity is high it is nearly fully inhibited by BKA. Only at low levels do the BKA-resistant rates become apparent. Among the three mutants of the negatively charged helix-terminating residues, the OxPHos activity is little changed in E45G but virtually fully inhibited in D149S and D249S.

The relation of the phosphorylation rate to the CAT binding allows estimation of the turnover of AAC in oxidative phosphorylation (Figure 6B). It shows to what extent the mutation has affected the catalytic capability of the AAC independent of the influence on the expression level in mitochondria. It is purely accidental that the turnover of wt AAC is at 100/min and so the values can be taken also as percentage as referred to wt. The turnover is decreased in all gly$^-$ mutants. This is particularly well defined in K38A and R152A where good levels of AAC are still found, whereas in K48A and D149S the very low levels of AAC cause some uncertainties in calculating the turnover. It is noteworthy that in the two gly$^+$ mutants, K179M and E45G, the "efficiency" of AAC in OxPhos is markedly increased.

Transport Activity of the Reconstituted AAC. To measure directly the transport activity of the AAC and its mutant forms, the carrier protein has to be solubilized and reconstituted in phospholipid vesicles. Measurement of the transport in mitochondria can be misleading since yeast mitochondria are fragile, the more so if they originate from the gly$^-$ mutant cells. Transport activity in the reconstituted vesicles is measured by the exchange of radioactive external [^{14}C]ADP or [^{14}C]ATP against internal ADP or ATP. For each rate determination the time progress of [^{14}C]ADP uptake into vesicles was measured using a specially constructed

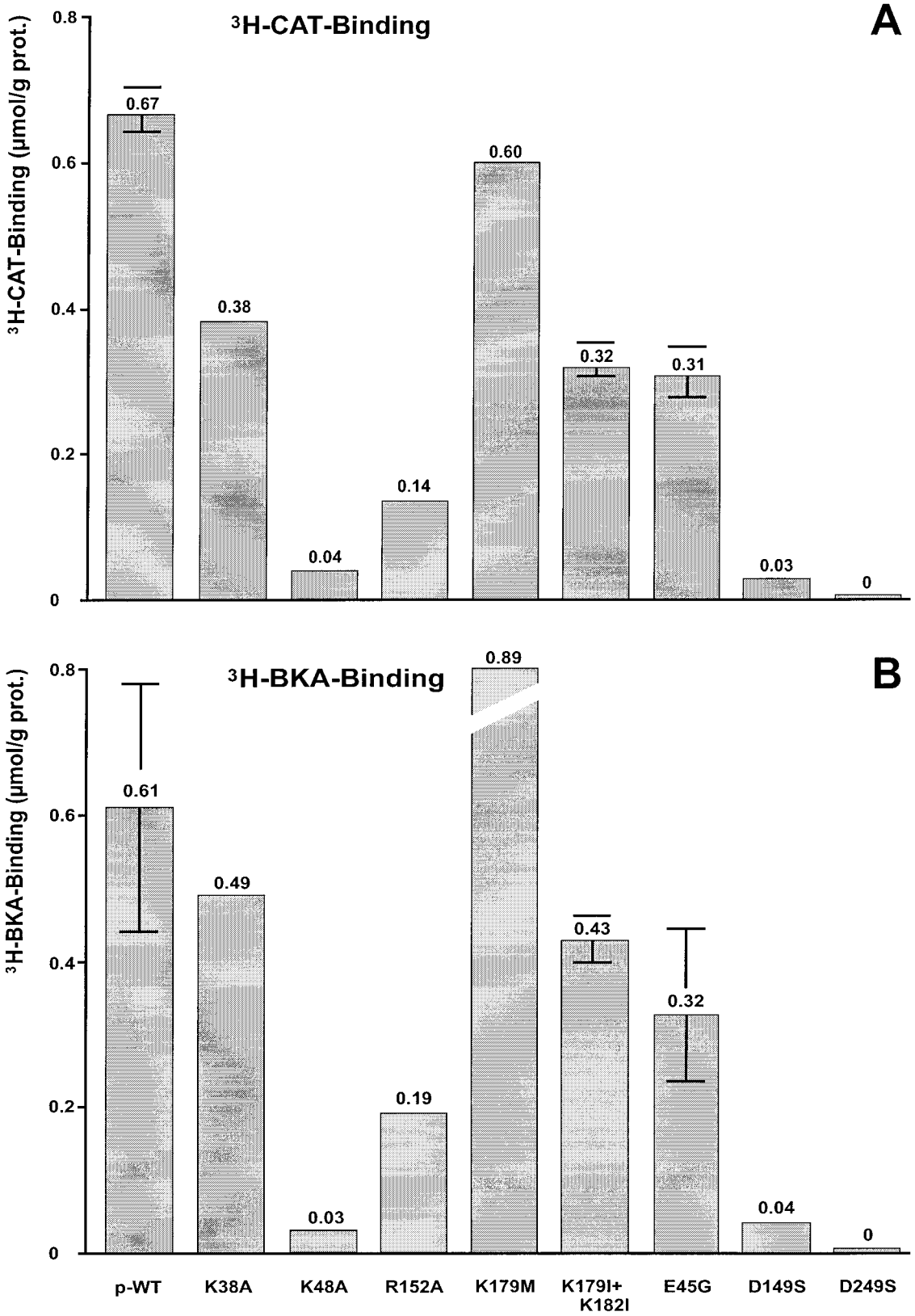

FIGURE 5: Binding of the specific AAC inhibitors CAT and BKA to mitochondria. (A) [^{3}H]CAT binding to mitochondria from various AAC mutants. (B) [^{3}H]BKA binding to mitochondria from various AAC mutants. The range encompasses two−three values from different mitochondrial preparations.

apparatus allowing automated mixing, sampling, and separation of the vesicles. The data were evaluated with a program according to a first-order rate equation (*9*). The rates of all four exchange modes were measured, i.e., ADP/ADP, ADP/ATP, ATP/ATP, and ATP/ADP. The values refer to the protein content present in the mitochondrial extract after passage through hydroxyapatite. The ionic conditions were optimized in the previous work and required KCl on both sides at equimolar concentrations. Under this provision the addition of valinomycin permitted relaxation of the charge differences accompanying the hetero exchange modes ATP/ADP and ADP/ATP.

The "basic exchange activity" of ADP/ADP exchange is reduced in the gly$^+$ mutants K179M and K179I + K182I to

Table 1: Oxidative Capacity of Mitochondria in Various AAC Mutants, Measured by the Respiratory Rate and Cytochrome *c* Content[a]

	respiration (μatom O/min/ g of protein)	cytochrome *c* content (μmol/ g of protein)	respiration cytochrome *c* $(\text{min})^{-1}$
p-wt	245 (202−293)	0.50 (0.30−0.65)	490
K38A	74 (65−84)	0.32 (0.25−0.37)	229
K48A	16	0.30 (0.26−0.33)	53
R152A	140	0.46 (0.24−0.68)	304
K179M	253 (245−262)	0.43 (0.30−0.57)	578
K179I + K182I	122 (78−170)	0.44 (0.36−0.51)	285
E45G	231	0.46 (0.35−0.59)	501
D149S	99	0.30 (0.29−0.30)	325
D249S	0	0.33	0

[a] The respiration is measured polarographically as described in Materials and Methods. For measuring the cytochrome *c* content, see Materials and Methods.

50% and 30% and in E45G to about 30% of wt activity (Figure 7). In the gly$^-$ mutants large differences are found. K38A has retained D/D exchange activity amounting to 10% of the wild type. Among the two homologoues in the matrix-located mutants, K48A is nearly completely inactive while R152A has still 40% of wt activity. Also strong contrasts occur among the helix-terminating residues. The reconstituted D149S and D249S AAC do not show any D/D exchange activity, while the homologue mutant E45G has more than 30% of wt activity.

The distribution of transport activity between the various exchange modes shows remarkably different patterns. Among the gly$^+$ mutants, K179M and K179I + K182I have a similar distribution between the exchange modes as the wild type, i.e., the exchange activities with external ATP, the T/T and the T/D modes, are the most active ones. They are more than twice as high as the exchanges with external ADP, such as the D/D and D/T modes. Differently, in the gly$^+$ E45G the T/D mode rate is lower than the T/T mode. A drastic change in the patterns of these four exchange modes as compared to the wild type is seen in gly$^-$ mutants whenever there is a measurable activity. On a widely varying level, the modes with external ADP (D/D and D/T) have higher activity than the modes with external ATP (T/D and T/T). This inverted pattern is best exemplified in R152A. Although the basic ADP/ADP exchange activity is nearly as high as in the gly$^+$ mutants, the near total suppression of oxidative phosphorylation is obviously related to the exchange mode inversion (EMI), as will be discussed below.

The sensitivity of the reconstituted transport toward the specific inhibitors CAT and BKA not only demonstrates that AAC is responsible for the observed activities but also allows discrimination of the direction of AAC insertion in the vesicles. CAT is membrane impermeant and specific for the c-side of the AAC, whereas BKA is specific for the m-side but permeant to the membrane (*1*). The inhibition has been assayed with the basic ADP/ATP exchange rate (Table 2). It is striking that CAT inhibits only to 8% in the wt and between 20% and 35% in the various mutants. The inhibition by BKA reaches between 60% and 88%. Nearly full inhibition is observed by the combination of CAT and BKA. The degree of inhibition by CAT alone indicates that 8−35% of the incorporated AAC is right-side out. In principle, it could be expected that BKA inhibits AAC inserted on the right or inversed side and thus completely inhibits the transport. This, however, is only true for the K38A and E45G mutant, whereas for unexplained reasons in K179M and K179I + K182I BKA does not fully inhibit and may not reach or bind all inhibition sites.

In order to illustrate the exchange mode inversion caused by the mutations, the differences of the two homo exchange modes (D/D − T/T) and the two hetero exchange modes (D/T − T/D) are plotted (Figure 8). These differences are related to the sum of all exchange modes in order to emphazise the mode shifts independent of the large absolute rate changes. For the D/D versus T/T exchange the inversion is clearly visible in the three gly$^-$ mutants. The relative differences are positive with the gly$^+$ wt and K179M, K179I + 182I, and E45G but negative for K38, K48A, and R152A. The inversion of the hetero modes T/D versus D/T is only seen in K48A and R152A.

DISCUSSION

Within our program to mutate conspicuously located charged residues in the AAC2 of yeast, the success rate of affecting the transport capacity of AAC has been unusually high. Previously we reported on the mutations of six arginine groups located within the second helix of each of the three repeat domains of the AAC2 and within three arginines in a triplet on the matrix site of the last domain (*8, 9, 12*). All of these mutations caused partial or complete loss of function. In this paper we have selected further five basic and three acidic residues. While the intrahelical K38A is characteristic for all AAC known so far, the other mutated residues are largely conserved also in other carriers of the family. In other words, only from K38A can we expect specific AAC-related effects whereas the mutational impact on the other residues should be interpreted in more generalized terms. Six of the nine mutations caused a partial or complete loss of AAC transport function. With this second set selection of charged residue mutations we have concluded this first approach to site-directed mutagenesis of AAC2.

The AAC Exclusive K38. K38A has an unusual position, being an intrahelical lysine and being AAC exclusive. Transmembrane intrahelical lysines are rare as compared to arginines which are better adapted to a low dielectric environment because of their delocalized positive charge. Early experimental evidence of a specific role of the corresponding K24 in the AAC from bovine heart came from probing with pyridoxal phosphate lysine groups from both sides of the mitochondrial membranes (*13*). Among the 10 out of the 22 lysines of the bovine AAC into which pyridoxal phosphate was incorporated, K24 was distinguished by a nearly complete protection by CAT against pyridoxal phosphate incorporation. This suggested that K24 is involved in binding of CAT and possibly also of ADP and ATP.

In agreement, mutation of K38A causes a major although not complete inactivation of AAC function. It is noteworthy that the expression level of K38A as measured by binding of the inhibitors CAT and BKA and by ELISA is still comparatively high which is different from other highly inactivated mutants. We relate this exception to the exclusive occurrence of K38 in AAC, while the other mutations are at residues widely conserved in the carrier family. Since these are probably important also for the structure and or the import of AAC to mitochondria, their elimination would depress or abolish the expression. Conversely, one may reason that because K38 has a more specific functional role in the AAC its elimination does not strongly depress expression.

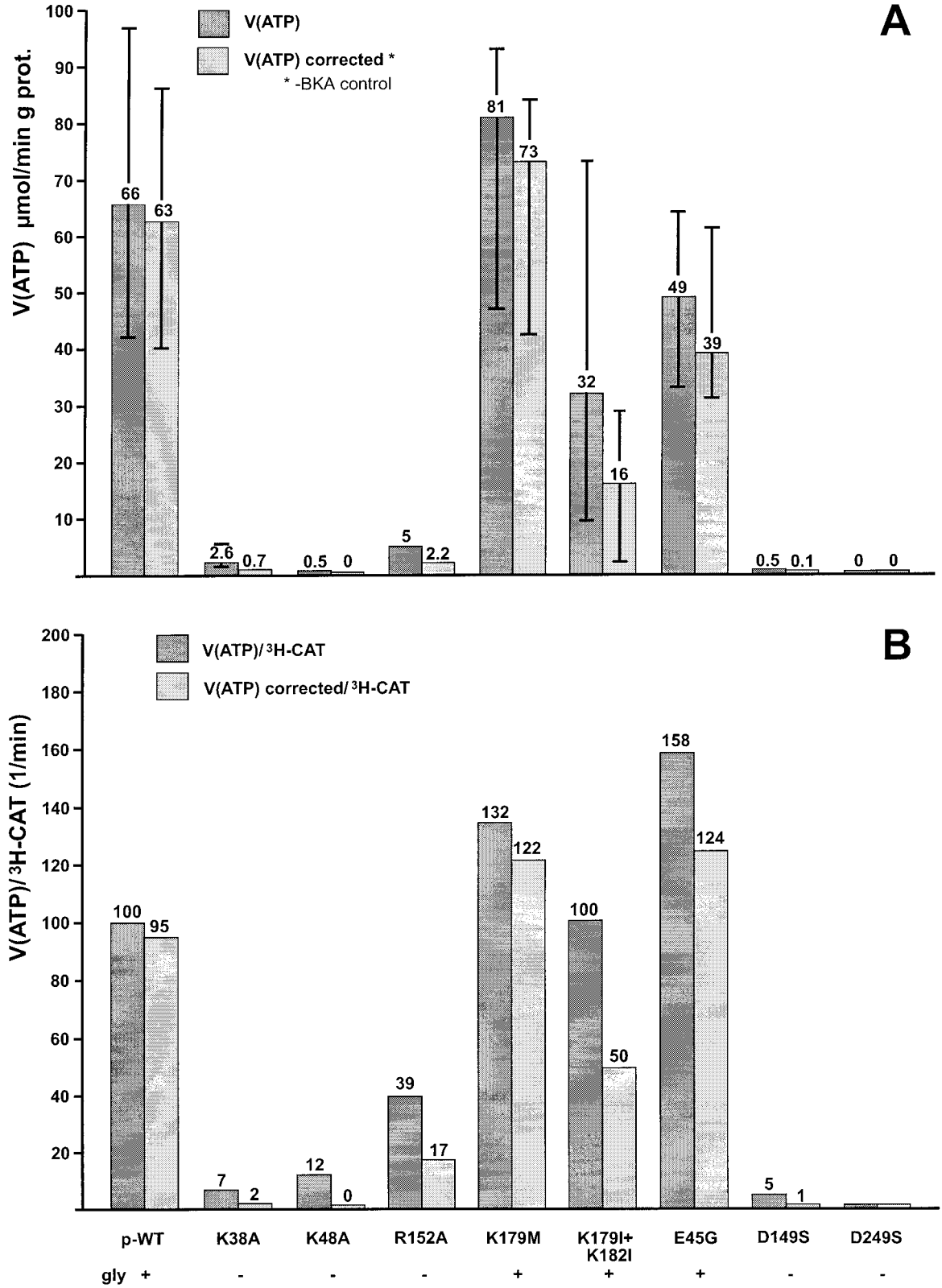

FIGURE 6: (A) Oxidative phosphorylation by isolated mitochondria of various AAC mutants. The ATP synthesis rates are evaluated from the time progress of ATP formation. The rates are given before and after correction for the BKA + CAT resistant rates. The range encompasses three−five measurements, and the mean value is given. For details see Materials and Methods. (B) Turnover of the AAC from different mutants. The turnover is calculated with the average values of *V*(ATP) and [^{3}H]CAT binding given in Figures 5A and 4A.

The calculated turnover number in oxidative phosphorylation of the K38A−AAC amounts to only 3% of the wild type activity. This extremely low phosphorylation rate seems at first to be at odds with the "basic" ADP/ADP transport capacity of the reconstituted K38A which still is about 16% of the wild type. The K38A is a typical case of the exchange mode inversion (EMI) with a preferential inhibition of the capability to transport ATP. It thus fits into the class of several previously described arginine mutants where the ATP-including modes are preferentially depressed (*9*).

Although from the pyridoxal phosphate incorporation studies a role of K38A in [^{3}H]CAT binding was predicted (*13*), there was no change in the capacity for CAT as well as for BKA binding. This would indicate that CAT covers

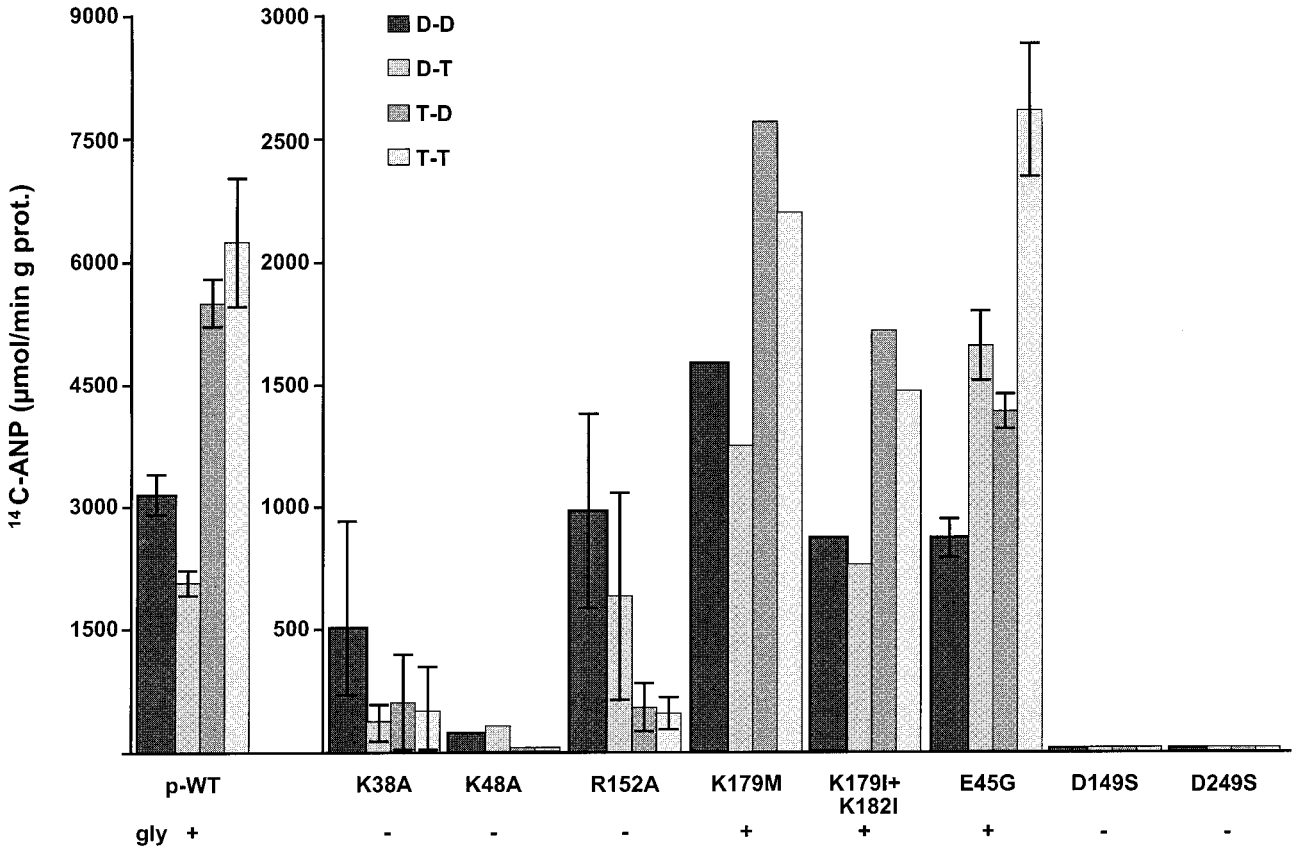

FIGURE 7: Exchange rates in reconstituted vesicles. The "basic" ADP/ATP exchange rate (D/D mode) and the other three exchange modes (D/T, T/D, T/T) are given. Measurements of up to four different preparations by the rapid removal stop method at 10 °C. For reconstitution and details of measurement procedure, see Materials and Methods.

Table 2: Inhibition by CAT and BKA of Basic ADP/ATP Exchange Activity in Proteoliposomes[a]

	% inhibition		
AAC	10 μM CAT	10 μM BKA	10 μM CAT, 4 μM BKA
p-wt	7	83	90
K38A	38	89	95
R152A	22	90	83
K179M	39	61	98
K179I + K182I	35	68	98
E45G	33	86	91

[a] The addition of the inhibitors of the vesicles were made 2 min before the start of the reaction. Three types of additions were made, 10 μM CAT, 10 μM BKA, and 10 μM CAT plus 4 μM BKA combined. The experiments were performed with the rapid removal technique at 10 °C.

up the access route to K38, rather than K38 providing a positive charge for binding the sulfate or carboxyl groups of CAT^{4-}.

The Matrix Triad Members K48 and R152. K48A and R152A are located in the motif (+x+) which occurs at a similar position in the three repeats on the matrix side between the two helices. Together with R252 they form a triad of basic residues at similar positions in each repeat domain. The thrice repeated motif (+x+) is generally conserved within the members of the mitochondrial carrier family. Within this triad most striking is the AAC-typical arginine triplet R252, R253, R254 in the last domain, where a replacement of each arginine by a neutral residue was previously shown to strongly suppress the translocation activity (*9*).

Both K48A and R152A mutants are fully devoid of cellular OxPhos. But R152A still sustains minor OxPhos activity in mitochondria. In the reconstituted system the "basic" exchange activity D/D of K48A has only 3% wt activity, whereas in R152A the transport activity is still half of wt AAC which is surprising in view of the low OxPhos. In both mutants the exchange modes including external ATP are drastically reduced. In K48A they are undetectable but in R152A, on the background of a high D/D activity, the rates of T/D and T/T exchange are still clearly measurable. In fact, R152A represents, similar to the previously described R294A mutant, a clear case of EMI where the basic exchange activity is largely retained but the ability to deal with external ATP is suppressed.

To explain the nearly complete suppression of OxPhos two factors have to be considered. First, as evidenced by the poor inhibition with CAT, in the reconstituted vesicles the AAC is largely inserted with the m-side outside, i.e., opposite to the situation in mitochondria where during OxPhos the m-side of AAC accepts ATP. This has to be taken into account if one compares in vesicles the rates of the much slower T/D mode with the D/T mode. The T/D mode is relevant for OxPhos in mitochondria. Further, in the competition for the total exchange capacity between the productive (T/D) and the unproductive (D/D, T/T) and counterproductive (D/T) modes the productive mode is suppressed. The simple formula

$$V_{\mathrm{OxPhos}} = k\gamma V_{\mathrm{T/D}}$$

with the competition coefficient

$$\gamma = V_{\mathrm{T/D}}/\sum(V_{\mathrm{D/D}}, V_{\mathrm{D/T}}, V_{\mathrm{T/T}})$$

might illustrate this competition. It would have to be refined

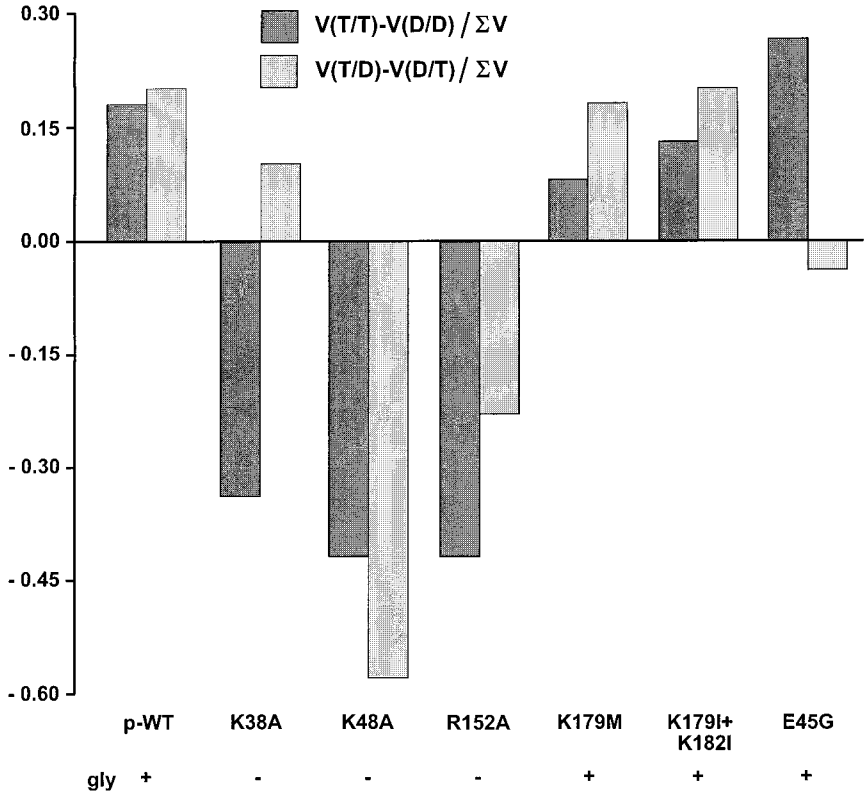

FIGURE 8: Illustration of the exchange mode inversion by the mutations. Relative rates are given to suppress the influence on the absolute rate. Negative values illustrate exchange mode inversion (EMI) as compared to wild type. The differences between the two homo exchange rates (T/T − D/D) and the two hetero exchange rates (T/D − D/T) are divided by the sum of all exchange modes. The average values of Figure 6 are used.

by the concentration ratios ATP/ADP inside and outside and the modulation by the membrane potential. The latter would superimpose a strong advantage to the productive mode (*17*, *18*). However, only if the coefficient γ is favorable enough can $\Delta\psi$ carve out a sufficiently high share for the productive exchange mode. This is not the case in the R152A and similar mutants, as it was in the previously studied R294A mutant (*9*), obviously due to the strong unproductive D/D mode competition.

Together with the previous mutations in the arginine triplet R252, 253, 254, the present K48A and R152A mutants demonstrate the importance of the matrix motif (+x+). Whether the motif is primarily involved in maintaining the structure is not clear yet. We had speculated that by forming positive charge rings these motifs are involved in attracting anions into the carrier vestibule (*19*). In this function they may also be part of alternating positively and negatively charged rings involved in propagating the anion through the protein (*20*).

K179 and K182. The mutations of K179 and K182 in yeast were motivated by pyridoxal phosphate labeling studies on bovine heart mitochondria (*13*). Although the homologous residues K162 and K165 belong to the matrix portion in the second repeat domain, they are accessible to the membrane impermeant pyridoxal phosphate from the c-side in mitochondria. Further, the reactivity with pyridoxal phosphate was dependent on the translocational state, i.e., it was labeled only from the c-side in the m-state of AAC. This suggested that the bovine K162 is involved in the translocational path. Contrary to these expectations the mutation K179I did not markedly decrease the transport activity of the AAC. OxPhos and growth characteristics are similar to the wild type. Actually it is the first case among our mutations of positive residues without a marked damage of translocation activity. Even in the double-mutant K179I and K182I the decrease in the OxPhos and transport activity was not strong enough to inhibit growth on nonfermentative substrates.

The Helix-Terminating Acidic Residue Triad, E45, D149, D249. According to our folding model of AAC2 the transmembrane helices are delimited by charged residues, in particular by negatively charged residues on both sides of the membrane. In each of the three domains the first helix is terminated by an acidic residue on the matrix side, E45, D149, and D249. These negative residues are quite well preserved within the mitochondrial carrier family (*12*) and can be expected to be important for the transmembrane structure since an elimination may destabilize the helix anchoring in the membrane. As three times repeated negative residues they may form charged rings which alternating with positively charged rings may participate in the propagation of the substrates (*20*).

The mutational neutralization of these residues has surprisingly divergent effects. Whereas in E45G OxPhos in cells and mitochondria is only little affected, in the corresponding mutation D149S and D249S in the second and third domain OxPhos is completely suppressed. The expression level of AAC is still half of wt in E45G and in D149S, and particularly in D249 lower levels of AAC are found. A more drastic degradation is seen for the exchange activity in the reconstituted system. E45G still retains 30% of wt activity whereas the D149S and D249S AAC are virtually fully incapacitated. Interestingly, the gly^+ E45G mutation has no exchange mode inversion routinely found in gly^- mutants, for example, in R294A and R152A. This shows again that more than the absolute decrease of the rates it is the EMI

Table 3: Asymmetry in the Triad Mutations[a]

localization	triad		
intrahelical	R96	R204	R294
	−	−	+
helix limiting	E45	D149	D249
	++	−	−
hydrophilic matrix region	K48	R152	R252
	−	+	−

[a] −, complete or near complete inactivation. +, retention of basic D/D activity, but gly$^-$ growth. ++, retention also of gly$^+$ growth.

which causes the cells to become gly$^-$, i.e. OxPhos insufficient.

The Triad Asymmetries. The contrast between the structural similarity of the positions of these three acidic residues and their drastically divergent importance for AAC function is a particularly striking example for a functional and possibly also structural asymmetry among the three repeat domains of the AAC. Similar asymmetries are observed by the mutations in two other triads. In the previously mutated intrahelical arginine triad, R96, R204, R294, the R294A mutation results in a nearly unchanged basic D/D exchange activity, while the R96A and R204 are knock outs. In a third triad encompassing the motif (+x+), located in the hydrophilic matrix region, the R152A mutation in the second repeat domain still allows for good transport activity, whereas the K48A and the single R252I mutation nearly fully inactivate the AAC. Thus, in each of the triads one member is comparatively resistant to neutralization of the charge (Table 3). In other words, within one triad the members of only two repeat domains are vital for function. They change their localization between the domains in a rotatory fashion. For the intrahelical triad the vital domains are 1 and 2, for the helix-limiting negatively charged triad domains 2 and 3, and for the hydrophilic matrix loop triad domains 1 and 3.

Mutational Abolition of CAT and BKA Binding. Among our present crop of mutants, the three mutants K48A, D149S, and D249S are the first cases where mutations largely suppress the capability to bind tightly the AAC-specific inhibitors CAT and BKA. Although there is a lower but significant expression level of the AAC protein in mitochondria, the binding of CAT and BKA is very weak. Also in the reconstitution system the AAC from those mutants does not exhibit any transport activity. The results are unexpected in several ways. First, we would have expected suppression of inhibitor binding by the elimination of positive charges, but in our previous crop of mutational positive charge neutralization, no evidence for a suppression of CAT binding was obtained. Only for the original op1 (pet9) mutant, which was later identified as a R96H mutant (*21*), an increase of the K_D for CAT had been previously determined (*22*). Second, the three residues found to be important for CAT binding do not follow any three-partite regularity. Two are negatively charged helix terminators and one is in the matrix side a member of the (+x+) motif. All groups face the matrix side. It remains unclear whether any of these residues is directly involved in the binding of CAT or BKA or whether their mutational changes indirectly disturb the binding pocket, which according to photoaffinity labeling involves the matrix segment of the third repeat domain (*23*). It is noteworthy that the same mutants have a near complete inhibition of transport activity. This agrees with the contention that CAT and ADP or ATP use overlapping binding centers in the AAC (*24*).

ACKNOWLEDGMENT

We thank Ilse Prinz for the preparation of mitochondria and Hendrik Schubert for the many large scale yeast cultures.

REFERENCES

1. Klingenberg, M. (1976) in *The Enzymes of Biological Membranes: Membrane Transport* (Martonosi, A. N., Ed.) Vol. 3, pp 383−438, Plenum Press, New York.
2. Riccio, P., Aquila, H., & Klingenberg, M. (1975) *FEBS Lett. 56*, 133−138.
3. Aquila, H., Misra, D., Eulitz, M., & Klingenberg, M. (1982) *Hoppe-Seyler's Z. Physiol. Chem. 363*, 345−349.
4. Saraste, M., & Walker, J. E. (1982) *FEBS Lett. 144*, 250−254.
5. Aquila, H., Link, T. A., & Klingenberg, M. (1985) *FEBS Lett. 212*, 1−9.
6. Hackenberg, H., & Klingenberg, M. (1980) *Biochemistry 19*, 548−555.
7. Lawson, J. E., Gawaz, M. P., Klingenberg, M., & Douglas, M. G. (1990) *J. Biol. Chem. 265*, 14195−14202.
8. Müller, V., Basset, G., Nelson, D. R., & Klingenberg, M. (1996) *Biochemistry 35*, 16132−16143.
9. Heidkämper, D., Müller, V., Nelson, D. R., & Klingenberg, M. (1996) *Biochemistry 35*, 16144−16152.
10. Nelson, D. R., Lawson, J. E., Klingenberg, M., & Douglas, M. G. (1993) *J. Mol. Biol. 230*, 1159−1170.
11. Zoller, M. J., & Smith, M. (1984) *DNA 3*, 479−488.
12. Klingenberg, M., & Nelson, D. R. (1995) in *Biochemistry of Cell Membranes* (Papa, S., & Toger, J. M., Eds.) pp 191−219, Birkhäuser Verlag, Basel.
13. Bogner, W., Aquila, H., & Klingenberg, M. (1986) *Eur. J. Biochem. 161*, 611−620.
14. Nelson, D. R., & Douglas, M. G. (1993) *J. Mol. Biol. 230*, 1171−1182.
15. Klingenberg, M. , Appel, M., Babel, W., & Aquila, H. (1983) *Eur. J. Biochem. 131*, 647−654.
16. Klingenberg, M., & Buchholz, M. (1973) *Eur. J. Biochem. 38*, 346−358.
17. Krämer, R., & Klingenberg, M. (1980) *Biochemistry 19*, 556−560.
18. Krämer, R., & Klingenberg, M. (1982) *Biochemistry 21*, 1082−1089.
19. Klingenberg, M. (1995) in *Progress in Cell Research* (Palmieri, F., Papa, S., Saccone, C., Gadaleta, M. N., Eds.) Vol. 5, pp 65−70, Elsevier Science, Amsterdam.
20. Klingenberg, M. (1993) *J. Bioenerg. Biomemb. 25*, 447−457.
21. Kolarov, J., Kolarova, N., & Nelson, N. (1990) *J. Biol. Chem. 265*, 12711−12716.
22. Kolarov, J., & Klingenberg, M. (1974) *FEBS Lett. 45*, 320−323.
23. Lauquin, G. J. M., Brandolin, G., Lunardi, J., & Vignais, P. V. (1978) *Biochim. Biophys. Acta 501*, 10−19.
24. Weidemann, M. J., Erdelt, H., & Klingenberg, M. (1970) *Eur. J. Biochem. 16*, 313−335.

BI971867L